Research Square

Preprints are preliminary reports that have not undergone peer review.
They should not be considered conclusive, used to inform clinical practice,
or referenced by the media as validated information.

How soil anaerobic nitrogen-transformation processes and rates respond to agricultural use and management intensity in the water-level fluctuation zone of Danjiangkou reservoir?

Xinghua Pang
Institute of Mountain Hazards and Environment, Chinese Academy of Sciences
Zetao Chen
Water Source Limited Liability Company of the Middle Route of South-to-North Water Transfer Project
Rui Zhang
Institute of Mountain Hazards and Environment, Chinese Academy of Sciences
Weijie Guo
Changjiang River Scientific Research Institute
Lequn Zhang
Water Source Limited Liability Company of the Middle Route of South-to-North Water Transfer Project
Chengyu Zhang
Water Source Limited Liability Company of the Middle Route of South-to-North Water Transfer Project
Baohua Zhang
Water Source Limited Liability Company of the Middle Route of South-to-North Water Transfer Project
Zhenhua Wang
Changjiang River Scientific Research Institute
Han Liu
Changjiang River Scientific Research Institute
Minghua Zhou
mhuazhou@imde.ac.cn

Institute of Mountain Hazards and Environment, Chinese Academy of Sciences

Research Article

Keywords: Water-level fluctuation zone, Nitrogen transformation, Fertilization, Excess dissolved nitrogen, Hydrological regime

Posted Date: November 26th, 2026

DOI: https://doi.org/10.21203/rs.3.rs-11335942/v1

License: This work is licensed under a Creative Commons Attribution 4.0 International License.
Read Full License

Additional Declarations: No competing interests reported.

How soil anaerobic nitrogen-transformation processes and rates respond to agricultural use and management intensity in the water-level fluctuation zone of Danjiangkou reservoir?

Xinghua Pang[1,2], Zetao Chen[3], Rui Zhang[1,2], Weijie Guo[4,5], Lequn Zhang[3], Chengyu Zhang[3], Baohua Zhang[3], Zhenhua Wang[4], Han Liu[4,5], Minghua Zhou[1,2*]

[1] Institute of Mountain Hazards and Environment, Chinese Academy of Sciences, Chengdu, 610041, PR China

[2] University of Chinese Academy of Sciences, Beijing, 100049, PR China

[3] Water Source Limited Liability Company of the Middle Route of South-to-North Water Transfer Project, Danjiangkou 442700, China

[4] Changjiang River Scientific Research Institute, Changjiang Water Resources Commission, Wuhan, 430000, PR China

[5] Key Laboratory of Changjiang River of Ministry Water Resources, Wuhan, 430000, PR China

*Corresponding author: Prof. Dr. Minghua Zhou

E-mail addresses: mhuazhou@imde.ac.cn

Abstract:

The water-level fluctuation zone of reservoirs serves as a critical hotspot for nitrogen transformation, yet the driving mechanisms of nitrogen release during initial impoundment under different cropping systems remain poorly understood. The present study investigated the effects of conventional fertilizer (MN), slow-release fertilizer (MP), and nitrification inhibitor (MQ) application on nitrogen release and transformation under varying fluctuation conditions. MP sustained soil NH4+-N release and supplied organic carbon, increasing soil organic carbon by 9.41%. This coupled carbon–nitrogen input was associated with 17.72% higher denitrification potential than conventional fertilization during early flooding. DNRA potential under MP increased by 85.71% at the mid-flooding stage relative to conventional fertilization, but declined by 81.40% relative to control group after 53 days of flooding. In contrast, MQ suppressed nitrification during early flooding, reducing soil NO_3^--N by 28.09% and maintaining a high NH_4^+-N environment that limited denitrification and favored N retention. Hydrological regime further modulated the dominance of various nitrogen pathways. Compared with continuous flooding, drying after short-term flooding enhanced denitrification potential and suppressed DNRA relative to continuous flooding, shifting N fate from DNRA-dominated retention to denitrification-dominated gaseous loss. At the soil–water interface, MP and MQ reduced NH_4^+-N concentrations in overlying water by 51.06% and 51.60%, respectively. and reduced total dissolved N relative to MN. These findings show that novel fertilizers mitigate aqueous N-release risk by regulating nitrification and the competition between denitrification and DNRA, while flood–drying transitions may enhance gaseous N loss.

Keywords: Water-level fluctuation zone, Nitrogen transformation, Fertilization, Excess dissolved nitrogen, Hydrological regime

1. Introduction

The water-level fluctuation zones (WLFZs) of reservoirs are highly managed aquatic-terrestrial ecotones that provide critical services such as flood control and water supply, while also profoundly influencing regional and even global carbon (C) and nitrogen (N) biogeochemical cycles (Bernardo et al., 2017; Yang et al., 2021). In many large reservoirs, including the Danjiangkou Reservoir, these zones are increasingly used for agricultural production during drawdown periods, subjecting soils to various fertilization regimes and management intensities (Zhang et al. 2024; Zhang et al. 2025a). Such agricultural use modifies soil C and N inputs and consequently dictates the ecological niche occupancy and metabolic performance of N-transforming microorganisms (Wu et al., 2023a). However, how agricultural use and management intensity interact with the inherent hydrological dynamics of WLFZs to regulate soil N transformation processes, rates, and N release to water and atmosphere remains poorly understood.

Although previous studies have recognized the critical role of the WLFZs in the N cycle, our understanding of N transformation process and rate as well as underlying mechanisms during the reservoir impoundment phase remain limited (Su et al., 2025; Yu et al., 2020). As a biogeochemical hotspot, the WLFZs is characterized by fluctuating redox conditions and a variety of competing nitrogen transformation processes, including nitrification, denitrification, anaerobic ammonium oxidation (Anammox), and dissimilatory nitrate reduction to ammonium (DNRA). These processes occur concurrently and interact with one another within the soil profile (Hao et al., 2025). The interplay of N transformation processes under fluctuating hydrological conditions ultimately dictate N partitioning among gaseous release to the atmosphere, soluble export to the water column, and soil retention as NH_4^+-N (Gao et al., 2022; Lee et al., 2023; Su et al., 2022). Previous studies have primarily focused on determining the rates of these processes in natural or semi-natural paddy field buffer zones, or on exploring their correlations with static environmental factors. However, i there is a lack of systematic understanding of how agricultural management reshapes

the competitive relationships among these pathways, and consequently alters nitrogen transformation rates and release patterns.

A key to probing such competitive dynamics lies in the measurement of excess dissolved N_2 (ΔN_2), the direct product of denitrification. Because denitrification and DNRA compete for the same NO_3^--N substrate under anaerobic conditions, ΔN_2 not only tracks denitrification activity but also illuminates the relative importance of the DNRA pathway in retaining N within the soil (Enanga et al., 2017). Yet, how ΔN_2 responds to environmental and microbial drivers in WLFZ soils under different agricultural management intensities has not been explored, limiting mechanistic insights into N transformation rates and release potentials in these heavily utilized ecosystems.

Previous studies have shown that the reservoir drawdown zone, as a unique ecological interface characterized by periodic flooding and drying, serves as a hotspot for N transformation and release (Cai et al., 2025; Yu et al., 2020). Coincidentally, the period of hydrological disturbances also coincides with a critical phase of agricultural activities involving fertilizer application. In agricultural management practices within the WLFZs, the release of soil nitrogen into the environment is primarily influenced by fertilization practices. Novel fertilizer types, such as conventional fast-release fertilizers, controlled-release fertilizers, and nitrification inhibitors, represent distinct strategies of N input regulation, altering the timing, speciation, and quantity of available N and associated C inputs (Wu et al., 2023a). Concurrently, variations in flooding duration and the alternating flooding-drying cycles caused by reservoir operations reshape the competitive landscape of microbial functional groups by driving changes in redox conditions and N speciation (Sanchez-Rodriguez et al., 2017; Zhang et al., 2023a). While the separate effects of fertilization or flooding on soil N transformations are well documented, there is a critical knowledge gap on how the coupled influence of agricultural management intensity and hydrological processes shapes microbial community responses, and how this ultimately manifests in ΔN_2 dynamics and N transformation and release potentials.

To address this gap, the present study investigated responses of soil N

transformation processes and rates as well as N losses to different agricultural-land uses and fertilizer types in the WLFZ of the Danjiangkou Reservoir, a typical agricultural-impacted fluctuating zone. The objectives were to: (1) evaluate different fertilization practices on soil N transformation processes and rates; (2) examine how flooding duration dynamically interacts with fertilization practices to regulate N transformation rates.

2. Materials and methods

2.1. Soil collection and preparation

The experimental soil was collected from the water-level fluctuation zone of the Danjiangkou Reservoir in Nanyang City, Henan Province, China. Sample site is characterized by gentle slopes along the reservoir bank, and cultivated land is relatively concentrated. The specific sampling location is shown in Fig. S1(a) (The red line indicates the management and protection boundary of the reservoir area, this line also corresponds to the reservoir water level at an elevation of 170 m). The sampling area was large. Therefore, a five-point sampling method was adopted. The collected soil samples were thoroughly mixed and stored in a refrigerator at 4 °C for subsequent analysis.

2.2. Potted plant incubation experiment

The experiment started in early May and ended in late August. This period coincided with the crop growing season in the water-level fluctuation zone of the Danjiangkou Reservoir. A pot experiment was conducted with eight treatment groups. Each group had five replicates, resulting in a total of 40 pots, and six groups involved flooding conditions, accounting for 30 pots. The treatments were broadly divided into two categories: with crop planting and without crop planting. The dominant cropping pattern around the Danjiangkou Reservoir is a wheat-maize rotation. Therefore, maize was selected as the test crop in this incubation experiment. Recently the application of new types of N fertilizers has become one of the dominant cropping practices in the water-level fluctuation zone. Therefore, considering the effects of different cropping patterns on soil N and P release, this study also incorporated two additional agricultural

practices: the application of a new slow-release N fertilizer (urea-ammonium N fertilizer) and the use of a nitrification inhibitor. These treatments were included alongside conventional N fertilizer application.

The potted plant setup is shown in Fig. S2. Considering the varying inundation conditions of the soil in the riparian zone at different elevations, the potted plant experiments were primarily divided into two treatments: flooding and non-flooding. Based on the water level fluctuations of the Danjiangkou Reservoir (Fig. S1(b)) and the number of flooded days at different drawdown zone elevations (Table S1), the cultivation experiment was designed at water levels of 160 m, 165 m, and 170 m. Considering the maize growth, the total duration of the potted experiment was set at 90 days. At the 160 m level, the average flooding duration was 53 days, while the 165 m level had an average flooding duration of 20 days. The 170 m level generally did not experience flooding. Additionally, considering the maize planting date and the onset of flooding, the start dates for long-term flooding (53 days) and short-term flooding (20 days) occur on the 30th day after corn planting. The specific experimental treatment group design based on the above content is shown in Table S2.

The average flooding depth in this study was 1.0 m. To better evaluate N and P release fluxes from soil and crops with flooded conditions, surface and bottom water samples were collected from different flooding treatment groups at various time points. Water samples were taken at different depths on days 1, 3, 5, 7, 10, 15, 20, 30, and 53 of the complete flooding experiment. A portion of the collected water samples was stored at 4°C for analysis of total N (TN), total dissolved N (TDN), and form-specific N (NH_4^+-N and NO_3^--N), along with physicochemical parameters including dissolved organic carbon (DOC), and pH.

Soil samples were collected from each treatment group at three time points: Day 1 (flooding), Day 20, and Day 53 (after flooding). Surface soil was collected at each sampling event. A portion of the soil samples was stored in a refrigerator at 4 °C. These samples were used to analyze changes in N forms and N transformation potential. The analyses covered three periods: before flooding, after flooding, and during the drying phase. The remaining soil samples were stored in a freezer at −20 °C. These samples

were used to analyze basic physicochemical properties, including soil C, and pH.

2.3. Analyses of soil and water properties

Soil physicochemical properties were analyzed based on the method described by Avery and Bascomb (1974). For soil, NH_4^+-N and NO_3^--N were both extracted using 2 $mol \cdot L^{-1}$ KCl, NH_4^+-N was measured at 485 nm using Nessler's reagent spectrophotometry, while NO_3^--N was assayed at 220 and 275 nm. The soil pH was determined using a pH meter. In addition, dissolved organic carbon (DOC) was assayed using a Continuous Flow Analyzer System. Available P (AP) was measured using the molybdenum–antimony anticolorimetric method with an ultraviolet spectrophotometer (UV-2450) at 700 nm. Determination of soil alkali-hydrolyzable N (AN) refer to Bushong et al. (2008).

TN and TDN concentration in the water samples were determined using spectrophotometric methods. TN and TDN concentration were measured by ultraviolet (UV) spectrophotometry after digestion with alkaline potassium persulfate, following the method of HJ 636-2012. NH_4^+-N in water samples was also determined using Nessler's reagent spectrophotometry, and NO_3^--N was assayed at 220 and 275 nm.

2.4. Dissolved N in water and soil main N transformation rates

The concentration of dissolved N in the surface water was monitored using a membrane inlet mass spectrometer (MIMS; Bay Instruments, LLC 22-004, USA). The specific principles and operating procedures are described in Text S1. The difference between the measured dissolved N concentration and the theoretical saturation concentration was defined as excess dissolved N (ΔN_2).

The potential rates of denitrification, anaerobic ammonium oxidation (Anammox), and dissimilatory nitrate reduction to ammonium (DNRA) in the water-level fluctuation zone soils were determined. For each treatment and sampling period, approximately 20 g of fresh soil was placed into a 250 mL wide-mouth bottle and 140 mL pure water was mixed. Subsequent steps followed the procedures described in Text S2. The incubation lasted for 8 h. Potential N transformation rates were calculated based on the abundances of $^{29}N_2$ and $^{30}N_2$. These abundances were divided by the incubation time and soil mass ($\mu mol/(g \cdot h)$).

149 *2.5. Statistical analysis*

150 All data from this experiment were analyzed using Excel 2021 and SPSS 25.0 for
151 ANOVA. Box plots and bar charts for water quality indicators, soil physicochemical
152 properties, and soil nitrogen transformation processes across different experimental
153 groups were generated using Origin 2024b; the significance markers in the figures were
154 determined based on the ANOVA analysis. In addition, the environmental response
155 process of ΔN_2 was modeled using structural equation modeling (SEM), with SEM
156 models constructed using SPSS Amos Graphics 24.0. Random forest analysis of ΔN_2,
157 linear regression analysis of various environmental indicators, and partial least squares
158 path modeling (PLS-PM) of the soil nitrogen transformation process were performed
159 using the "randomForest," "dplyr," and "plspm" packages in R 4.4.3, respectively.
160

161 # 3. Results

162 *3.1. Fertilizer effect on soil properties*

163 Compared to conventional fertilizer, the application of novel fertilizers
164 significantly altered the concentrations of available N in the soil (Table S3). Compared
165 to conventional fertilizer (MN), the novel fertilizers—slow-release fertilizer (MP) and
166 nitrification inhibitor (MQ)—significantly decreased soil NO_3^--N concentrations during
167 the initial flooding stage (by 5.17% and 28.09%, respectively). In contrast, after 53 days
168 of flooding, soils under MP and MQ exhibited significantly higher NO_3^--N than MN
169 (increases of 65.96% and 112.5%), indicating a delayed nitrification or reduced
170 denitrification loss. Notably, MP significantly increased soil organic carbon (SOC) by
171 9.41% at the final stage. This indicates that sustained-release coating materials can
172 significantly increase soil carbon input.

173 Flooding duration exerted dominant control over soil N speciation. As flooding
174 progressed from 0 to 20 days, soil NH_4^+-N and alkali-hydrolyzable N (AN) increased
175 (by 545% and 32.5%, respectively), while NO_3^--N was significantly decreased. In
176 contrast, after 53 days flooding, soil NH_4^+-N decreased by 26.0% relative to the mid-
177 flooding peak, whereas NO_3^--N was continued decreased (by 68.03%). Compared with

long-time flooding soil, the accumulation of NO_3^--N and NH_4^+-N was significantly higher in flooding-to-drying transition soil.

3.2. Fertilizer effect on N release at the water-soil interface

Fertilizer type significantly influenced N release to the overlying water (Fig. 1). Compared to MN, both MP and MQ significantly decreased water NH_4^+-N concentrations by approximately 51% throughout the flooding stage, and decreased total dissolved N (TDN) by 18.81% and 11.13% during the final stage, respectively. These reductions were accompanied by lower NO_3^--N in MP and MQ treatments. In contrast, dissolved organic N (DON) gradually increased with flooding duration, with its proportion rising 6.6-fold by day 20 and 6.7-fold by day 53.

As flooding duration increased, the concentrations of NO_3^--N, TDN, and TN concentration in the water showed a trend of initial decrease followed by an increase (Fig. 1 and Fig. S3). NO_3^--N concentrations decreased by 84.79% during the first 20 days flooding, followed by a 95.94% increased at day 53. As flooding duration progressed, the concentrations of NH_4^+-N, pH, and DOC in the water column exhibited a gradual increasing trend. In comparison to the initial flooding stage, the average DOC concentration at the final flooding stage showed a substantial increase of 24.82 mg/L. Additionally, the type of fertilizer applied significantly influenced the composition of N species in the water (Fig. S4).

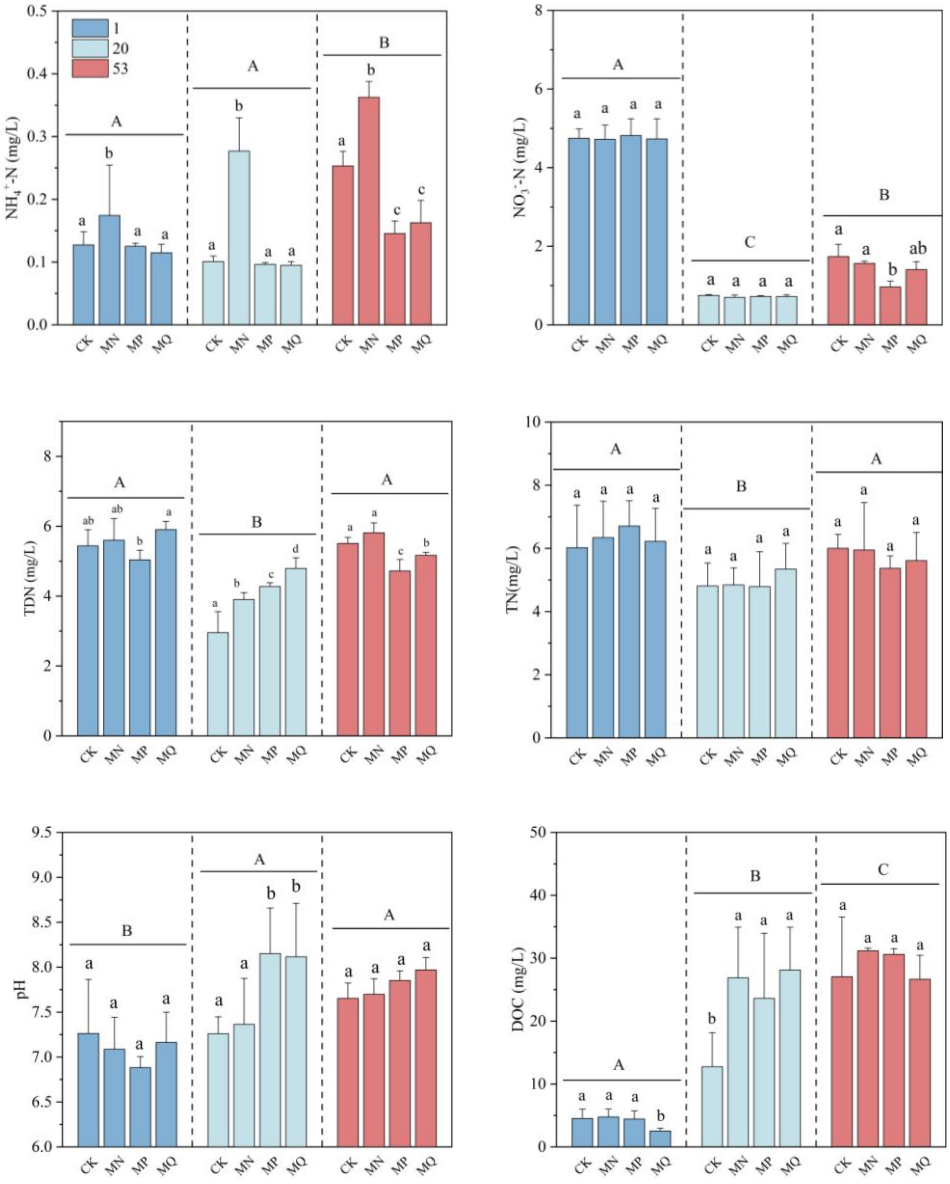

Fig. 1 Effects of different fertilization types on water properties during the initial (1d), middle (20d), and final (53d) flooding stages. Different letters indicate significant differences ($P < 0.05$). Lowercase letters indicate differences among fertilization treatments, while uppercase letters indicate differences among different flooding stage.

3.3. Dynamics of excess dissolved N_2 concentration

Following flooding, the range of excess dissolved N_2 (ΔN_2) concentrations in overlying water with different fertilization was approximately 34.99 ± 2.22 to 169.23 ± 18.02 μmol/L (Fig. 2(a)). During the initial flooding stage, novel fertilizers (especially MQ) significantly elevated ΔN_2 compared to MN, with MQ showing the highest peak

(168.45 μmol/L) and MN the lowest (92.56 μmol/L). However, after 7–15 days of flooding, ΔN_2 dropped to consistently low levels (34.99–79.01 μmol/L) across all treatments.

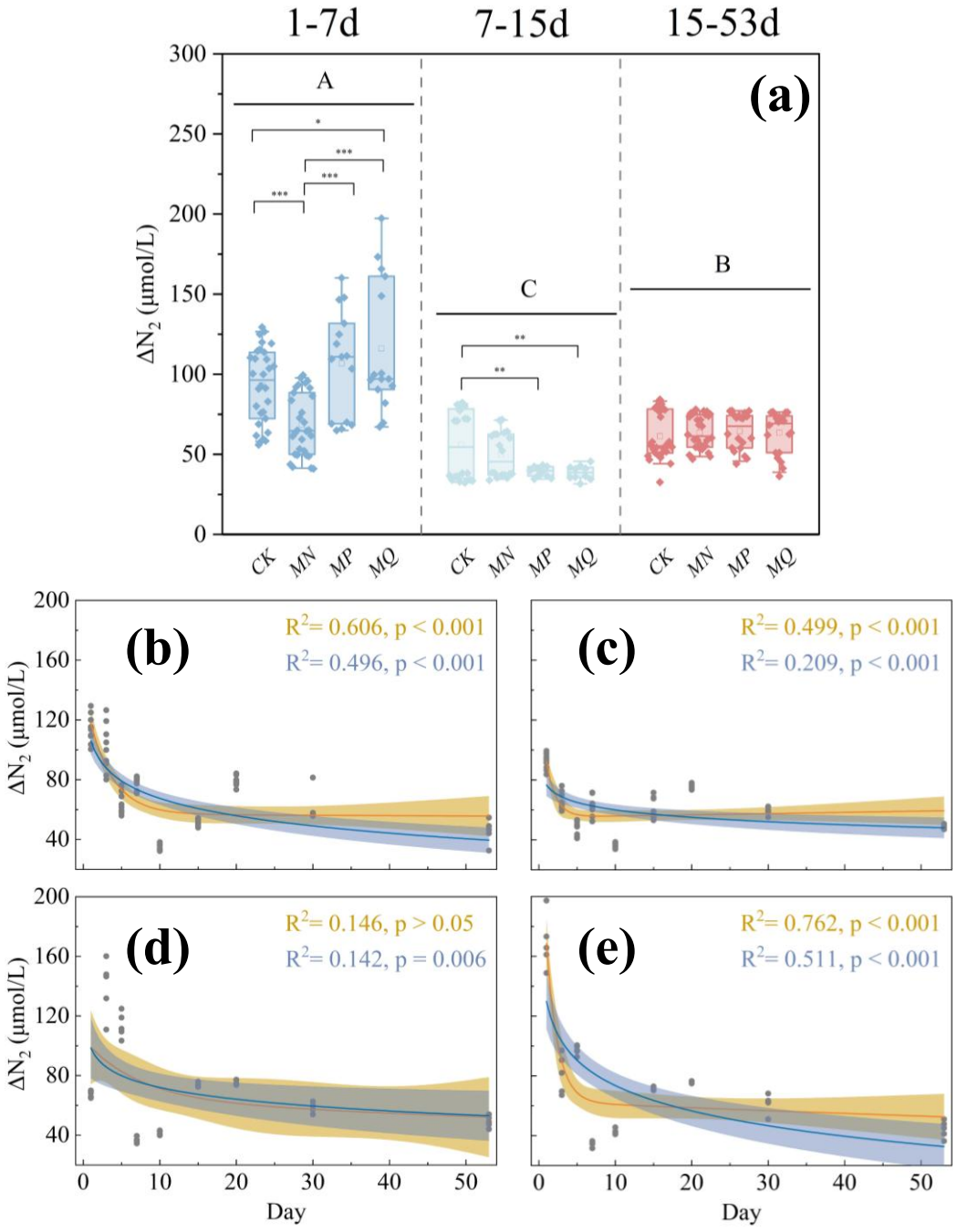

Fig. 2 Temporal dynamics of ΔN_2 concentrations across fertilization treatments. (a) shows ΔN_2 concentrations during initial, mid, and final flooding stages of each treatment. * $P < 0.05$, ** $P < 0.01$, ***$P < 0.001$. (b)-(e) present linear fits of ΔN_2 with flooding duration for CK, MN, MP, and MQ, respectively. Yellow and blue plots/text indicate logarithmic and double-exponential linear fit image/parameters.

As flood duration varied, ΔN_2 concentrations across all groups showed an overall decreasing trend (Fig. S5). To further investigate how ΔN_2 in water changed over time under different fertilization, we performed both logarithmic and double-exponential linear fits of time versus ΔN_2 (Fig. 2(b–e)). It can be observed that CK, MN, and MQ were better suited for double-exponential linear fitting, while the MP was better suited for logarithmic linear fitting. Comparing the linear fitting parameters, theoretically, during the initial flooding stage, MQ exhibited the highest maximum ΔN_2 (168.45 μmol/L), whereas MN showed the lowest (92.56 μmol/L) (Table S4). Additionally, during the initial flooding stage. MQ exhibited a faster rate of decrease in ΔN_2. In contrast, during the middle and final flooding stages, MN showed an increase in ΔN_2, while the ΔN_2 concentrations in the other treatment gradually decreased.

3.4. The responses of ΔN_2 to fertilization and flooding time

Random forest and structural equation modeling (SEM) consistently identified water NO_3^--N as the primary positive driver of ΔN_2, followed by fertilizer type, flooding time, DOC, and DON (Fig. 3, Fig. S6). Based on the partial dependence plots of different factors on ΔN_2, ΔN_2 increased with rising NO_3^--N and TN concentration, while decreased with increasing DOC concentration. Notably, when DON < 0.5 mg/L, ΔN_2 concentration increased with DON concentration; while DON > 0.5 mg/L, ΔN_2 gradually decreased.

Consistently, path analysis underscored the dominance of NO_3^--N in affecting ΔN_2 (Fig. 3). Flooding time plays a crucial role in regulating the response of ΔN_2 to NO_3^--N by influencing the concentration of NO_3^--N in water. The application of nitrification inhibitors also significantly affects NO_3^--N. Furthermore, DOC concentration similarly exert important roles in regulating ΔN_2. Specifically, flooding duration exerts a significant positively effect on ΔN_2 via DOC, while negative influences on ΔN_2 via concentration. Furthermore, the regulatory factors of ΔN_2 varied markedly among fertilization treatments. Under the unfertilized treatment, ΔN_2 was positively regulated by NO_3^--N (Fig. 3a). In contrast, conventional fertilization resulted in a significant positive correlation between ΔN_2 and DOC (Fig. 3b). Under the novel fertilizer treatment, both NO_3^--N and DOC exerted significant positive effects on ΔN_2.

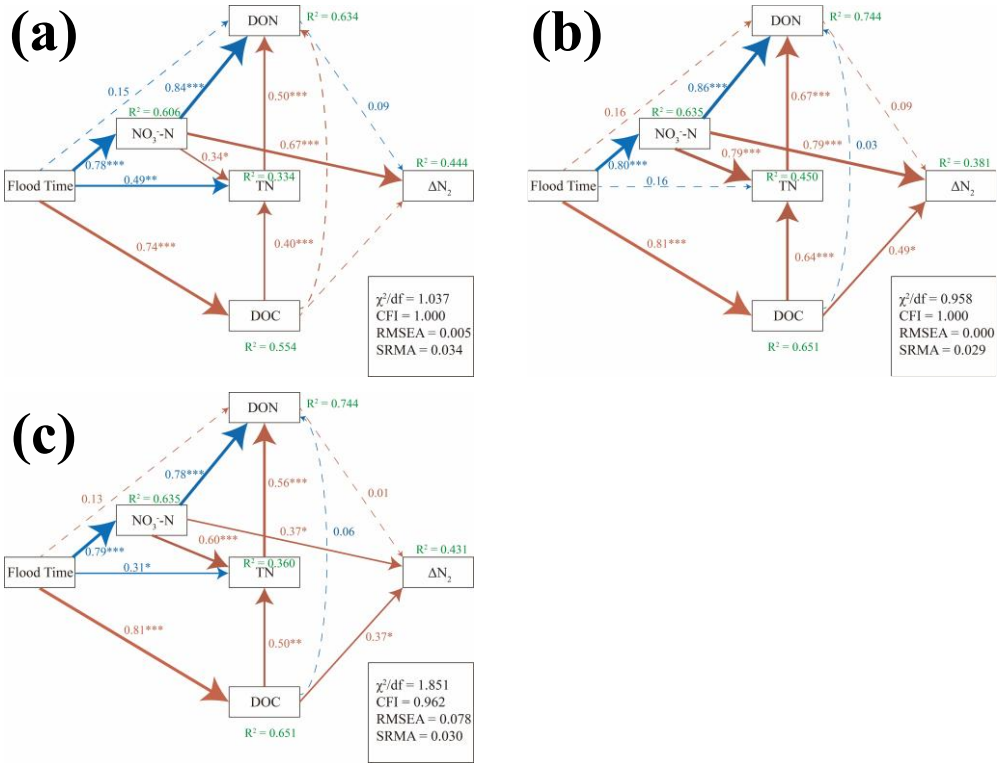

Fig. 3 Structural equation models (SEMs) illustrate the effects of (a) no fertilization, (b) conventional fertilization and (c) novel fertilization (controlled-release fertilizers and nitrification inhibitors) on various water quality indicators and ΔN_2. Numbers beside arrows represent standardized path coefficients, with arrow width scaled proportionally to path coefficients. * $P < 0.05$, ** $P < 0.01$, *** $P < 0.001$. Blue and orange arrows denote negative and positive correlations, respectively. Dotted lines indicate paths without statistical significance ($P > 0.05$). χ^2/df denotes the chi-square degrees of freedom ratio, GFI represents the goodness-of-fit index, and RMSE indicates the root mean square error of the model.

3.5. Fertilizer and flooding effect on soil N transformation rates

The average denitrification potentials of MP and MQ were higher than MN during the initial flooding stage (Fig. 4). During the initial flooding stage, fertilized treatments (especially MQ) exhibited higher denitrification and Anammox potentials than CK, while DNRA was suppressed. Specifically, the denitrification potential under MP was 17.72% higher than MN during the initial flooding stage. By the mid-flooding stage (day 20), denitrification and Anammox rates were significantly decreased, whereas DNRA rates increased significantly, and DNRA rates under MP was 85.71% higher than MN. This is consistent with its relatively high soil organic carbon (SOC)

content and sustained NH_4^+-N release. At the final flooding stage, denitrification and Anammox rates increased in MN but remained significantly lower in MP and MQ. While DNRA in fertilized soils was consistently suppressed relative to CK (MPL 81.40% lower than CKL). Notably, drying after short-term flooding significantly excessed both non-flooded and long-term flooded soil ($P < 0.05$). It suggesting that short-term flooding followed by drying enhances denitrification potential, independent fertilization status. Compared to long-term flooding, DNRA rates were markedly suppressed after short-term flooding followed by drying. Interestingly, although the soil Anammox potential in short-term flooding was not significantly different from long-term flooding or no flooding, Anammox potential of fertilized soils was significantly higher than CK. It was contradicted the trend to long-term flooded and unflooded soils.

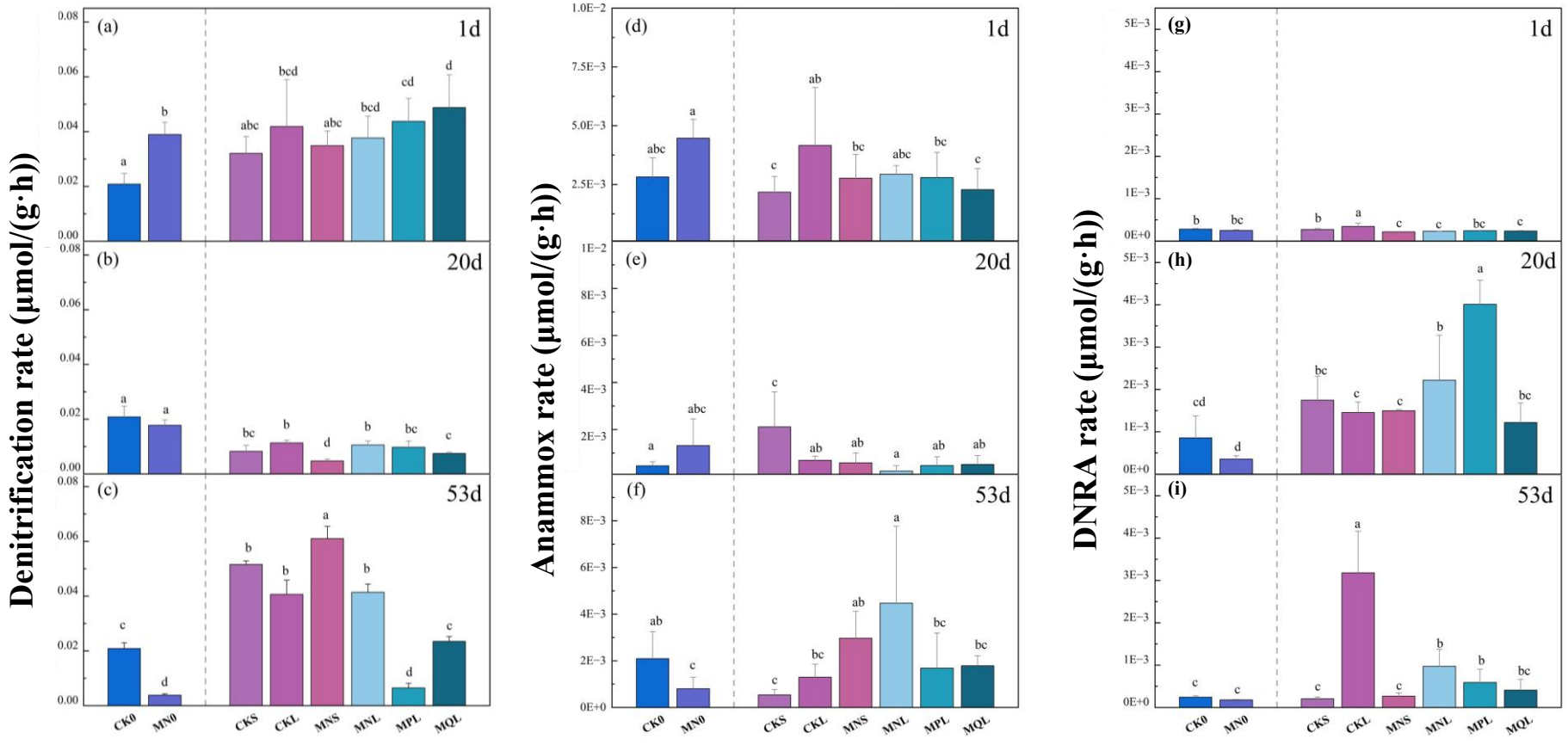

Fig. 4 Effects of different fertilization types on denitrification (a-c), Anammox (d-f) and DNRA (g-i) during the initial (a, d and g), middle (b, e and h), and final (c, f, and i) flooding stages. Different letters indicate significant differences ($P < 0.05$).

4. Discussion

4.1. Effects of Different Fertilization Practices on N Release at the water-soil interface

Our research findings indicate that controlled-release fertilizers and nitrification inhibitors can significantly decreased the release of N and P compounds such as NH_4^+-N, and TDN concentration in water during flooding (Fig. 1). Compared to conventional fertilizers, controlled-release fertilizers and nitrification inhibitors primarily regulate N transformation processes in the riparian zone soil, and influencing the risk of N and P release into water. Nitrification inhibitors primarily function by targeting and suppressing the activity of ammonia-oxidizing bacteria (AOB), and downregulating the abundance of AOB-amoA functional genes (Feyisa, 2026; Wang et al., 2024). This inhibits the biological oxidation process converting NH_4^+ to NO_3^-, significantly reducing soil NO_3^--N concentrations during the initial flooding phase. Recent studies further confirm that DMPP specifically targets nitrification-promoting microbial communities within the *Nitrosomonaceae* family and *Nitrospira* phylum (Vega-Mas et al., 2025). The biological inhibition effect of DMPP exhibits a phased characteristic. As flooding duration increases and anaerobic persist, the inhibitory effect diminishes (Wang et al., 2025). Persistently present NH_4^+-N in the soil gradually converts to NO_3^--N during the final flooding stage. In contrast, controlled-release fertilizers primarily regulate the timing of nutrient release. Their physical coating delays urea hydrolysis and NH_4^+ release rates while directly inhibiting ammonia-oxidizing microorganisms (AOA/AOB) and the expression of key genes (amoA, hao, etc.) (Gao et al., 2021; Miao et al., 2025). This indirectly limits substrate availability for nitrification. This explains why ΔN_2 dynamics under MP treatment better fit a log-linear model, while MQ aligns more closely with a double-exponential decay model.

Furthermore, the organic coating material in controlled-release fertilizers decomposed under flooded conditions, significantly increasing SOC (Table S3). This carbon-N coupling effect promoted heterotrophic DNRA processes during the middle-flooding stage (Fig. 4), potentially related to the specific carbon source type supplied by the controlled-release fertilizer (Cui et al., 2026). Wu et al. (2023b) research

indicates that the organic components of controlled-release fertilizers may promote fermentation processes, generating more available electron donors (e.g., acetate) that support DNRA processes under specific redox conditions. However, the concurrently elevated organic carbon environment may inhibit the organic carbon-sensitive Anammox process (Zhang et al., 2024), resulting in significantly lower Anammox potential in the controlled-release fertilizer compared to conventional fertilizer during the final flooding stage. Notably, both novel fertilizers decreased water NO_3^--N and NH_4^+-N concentration. However, while the carbon input effect of controlled-release fertilizers enhances soil carbon pools, it may also regulate the competitive relationship between denitrification and DNRA through carbon-N coupling. This could increase *nrfA* gene abundance and its correlation with NH_4^+-N, thereby influencing the N fate. (Gao et al., 2022; Jariwala et al., 2022). Interestingly, consist with Wu et al. (2023b) findings, during soil flooding, a high C/N ratio promotes the potential for denitrification and anammox while suppressing the DNRA potential (Fig. S7(c, g, and k)). The preferential allocation of readily degradable organic carbon to meet electron donor demands under high C/N ratios is a key factor driving denitrification and anaerobic ammonium oxidation. This shift in metabolic pathways is corroborated by an increased abundance of *nirS/K* and *hzsB* genes, while the concurrent suppression of *nrfA* expression highlights the greater sensitivity of the DNRA pathway to carbon source type (Gao et al., 2022; Zhang et al., 2023b; Zhang et al., 2025b).

Notably, during the late stage of flooding under the new fertilizer treatment, the observed shift from denitrification/anammox to DNRA was primarily governed by the speciation of dissolved inorganic N (DIN) and its coupling with the redox environment (Fig. S7(a, e and i)). The sustained release of NH_4^+-N from novel fertilizers, particularly controlled-release fertilizers, led to its accumulation in the soil (Yu et al., 2024). Product feedback inhibition, induced by the high soil NH_4^+-N concentration, weakens the driving force for further oxidation (Ye et al., 2021). Meanwhile, this NH_4^+-N -rich condition sustains DNRA by supplying its requisite substrate (Jariwala et al., 2022). Denitrification is constrained by insufficient NO_3^--N supply due to nitrification inhibition and competition for the common substrate NO_3^--N between DNRA and other

processes (Jiang et al., 2023; Wu et al., 2023b). Anammox also faces challenges, as it not only requires the coexistence of NH_4^+ and NO_2^- but also depends on a continuous supply of the substrate NO_2^-. The substrate supply for anammox is disrupted in high DIN and SOC environments. This is primarily attributed to two concurrent factors: (1) the competitive consumption of NO_2^- by heterotrophic denitrifiers (Wang et al., 2022), and (2) the intrinsic metabolic trait of DNRA that bypasses NO_2^- accumulation (Valiente et al., 2022). The novel fertilizer induces a shift in soil N transformation pathways from gaseous-loss-dominated processes (denitrification and Anammox) to N-conserving DNRA. This shift is driven by the fertilizer's modulation of DIN speciation and release patterns, in conjunction with the strongly reducing environment resulting from sustained flooding and organic carbon supply. Moreover, elevated NH_4^+-N and NH_4^+-N /TN in soil hindered the reduction of NO_2^- to N_2 (Maharjan et al., 2023), and suppressing the denitrification-dominated process of soil N release (Fig. S7(b, d)).

4.2. Effects of Flooding Duration on N Release at the water-soil interface

The temporal dynamics of N forms during the initial flooding stage are primarily reflected in the rapid decline of NO_3^--N in water (Fig. 1). In the newly formed anaerobic environment, NO_3^--N acts as the terminal electron acceptor, triggering intense denitrification at the soil-water interface. This process rapidly consumes NO_3^--N at a rate that surpasses any concurrent nitrification. Consequently, a net depletion of NO_3^--N is observed in the overlying water (Du et al., 2024). Additionally, under anaerobic conditions, the reductive dissolution of iron/manganese oxides releases exchangeable NH_4^+-N, coupled with the ongoing anaerobic mineralization of soil organic N (Lian et al., 2023; Liu et al., 2018). With nitrification suppressed, NH_4^+-N accumulates temporarily in the soil as it becomes the terminal product of these mineralization processes. However, soil NH_4^+-N concentrations decreased by 26.00% during the late inundation phase compared to the middle stage, as adsorption-desorption equilibrium was gradually approached. Concurrently, the activation of anaerobic NH_4^+-N consumption pathways curtailed further net accumulation. The initial stage of NH_4^+-N release primes subsequent N transformations and constitutes a significant reservoir for potential N release upon soil re-aeration (Fig. 5(a-c)) (Yu et al., 2020). Concurrently,

the decay of crop residues, such as maize, enhances the potential for N removal via Anammox and denitrification, thereby activating multi-pathway N cycling during the subsequent dry stage (Xu et al., 2026).

The sustained increase in DON concentration during flooding represents a shift in N speciation. This increase enhances microbial processes such as organic N mineralization and denitrification, thereby reflecting heightened microbial activity rather than passive accumulation (Qiu et al., 2024). Under prolonged anaerobic conditions, the release of DON becomes predominantly coupled with the decomposition of soil organic carbon and crop residues, shifting from the initial physical dispersion that dominates during early flooding (Fadum et al., 2025). This biologically derived DON originates from microbial cell lysis, extracellular enzyme activity, and microbial residue turnover (Du et al., 2024). As denitrification and Anammox processes deplete dissolved inorganic N (DIN) pools, the relative dominance of DON precisely reflects the transformation of inorganic N into complex organic compounds by active microbial communities (Lv et al., 2022).

For short-term flooding soils, the transition from flooded to dry exerts a significant stimulating effect on soil N transformation pathways. This effect exhibiting distinct differentiation across various biogeochemical processes. Cohen's d analysis (Table S5) and PSL modeling (Fig. S8) indicate that post-drying soil exhibits heightened sensitivity in NO_3^--N, NH_4^+-N, denitrification, and DNRA potential. Correspondingly, soil denitrification potential exhibited a pronounced priming effect during the post-flood drying stage. This is attributed to the NO_3^--N accumulation during the drying stage, which provided an ample substrate reserve and increased the abundance of denitrification genes such as *nirK* (Riya et al., 2017; Yu et al., 2020). Notably, even under aerobic conditions at the time of sampling, the soil's biogeochemical potential had been fundamentally altered by the preceding flood-dry cycle (Sao et al., 2024). PLS analysis identified soil NH_4^+-N content as a critical regulator of denitrification and DNRA potential (Fig. 4 and S7). The post-flood drying stage enhances denitrification by alleviating NH_4^+-N -induced inhibition of denitrifying bacterial activity (Liu et al., 2019; Yu et al., 2020), as evidenced by the observed reduction in soil NH_4^+-N during

drying stage (Fig. S9). Conversely, disruption of the strictly anaerobic conditions required for DNRA, and competitive utilization of its substrate NO_3^--N by aerobic/facultative denitrifying bacteria such as Pseudomonas better adapted to oxidative conditions (Cheng et al., 2022; Duan et al., 2023). Notably, TN concentration exerted no significant effect on either denitrification or DNRA (Fig. S8), indicating that the organic N pool participates in regulation indirectly, primarily through mineralization to inorganic forms. Consequently, the metabolic regime of microbial functional groups shifts from DNRA-dominated NH_4^+-N accumulation under prolonged flooding to denitrification-dominated NO_3^--N consumption after drying.

4.3. Regulation of excess dissolved N_2 by substrate competition between denitrification and DNRA

As a direct product of denitrification, ΔN_2 comprehensively reflects the combined effects of fertilizer management and flooding conditions on N transformation activity (Laursen and Seitzinger, 2002). The synergistic effects of carbon-N coupling in controlled-release fertilizers and substrate retention by nitrification inhibitors underlie the distinct ΔN_2 patterns between fertilizer types—particularly the elevated initial-flooding ΔN_2 in new-type fertilizer treatments. Specifically, Controlled-release fertilizers inhibit urease activity and downregulate N-transforming genes such as *amoA* and *norB*, thereby reducing NH_4^+-N loss. At the same time, controlled-release fertilizers increase the content of active SOC in the soil, indirectly stimulating microbial denitrification (Jariwala et al., 2022; Miao et al., 2025). Concurrently, nitrification inhibitors suppressed nitrification, reducing NO_3^--N leaching and N_2O production, thereby retaining N in the soil as NH_4^+-N for subsequent denitrification (Lam et al., 2017; Liu et al., 2025; Woodward et al., 2021). Random forest analysis (Fig. S6) identified NO_3^--N as the primary driver of ΔN_2 (Chen et al., 2020). By preventing NO_3^--N loss via leaching or excessive denitrification following application, these complementary mechanisms ensure NO_3^--N availability during the initial stages (Bordoloi et al., 2020; Khan et al., 2017).

Environmental factors regulate ΔN_2 primarily by influencing the competitive allocation of soil and water NO_3^--N among different microbial reduction pathways (Fig.

5(d)) (Jia et al., 2020). NO_3^--N is a common substrate for both denitrification and DNRA. Its availability dictates substrate allocation between these competing pathways, thereby governing total N transformation fluxes and the magnitude of ΔN_2 production (Deng et al., 2024; Jia et al., 2020). Similarly, the negative regulatory effect of DOC reflects the selective role of electron donors in NO_3^--N reactions (Sun et al., 2021). Elevated DOC concentrations stimulate heterotrophic activity, shifting the partitioning of NO_3^--N from denitrification toward DNRA. In addition, water DON serve as an indicator of N source modulation: low concentrations reflect rapid mineralization that replenishes the NO_3^--N pool (Wu et al., 2020), whereas high concentrations signal a microbial shift toward N retention strategies (Yang et al., 2025). Furthermore, as the end product of DNRA, NH_4^+-N accumulated in soil may exert indirect feedback control on NO_3^--N reduction pathways by modulating the expression of N-metabolism-related genes, such as *nrfA* (Pang and Ji, 2019). Therefore, NO_3^--N availability determines the intensity of substrate competition, DOC supply regulates the competitive capacity of fermentative DNRA bacteria, DON concentration thresholds indicate shifts in microbial metabolic strategy, and NH_4^+-N accumulation reinforces DNRA niche occupancy through positive feedback regulation (Pang and Ji, 2019; Wu et al., 2020; Yang et al., 2025).

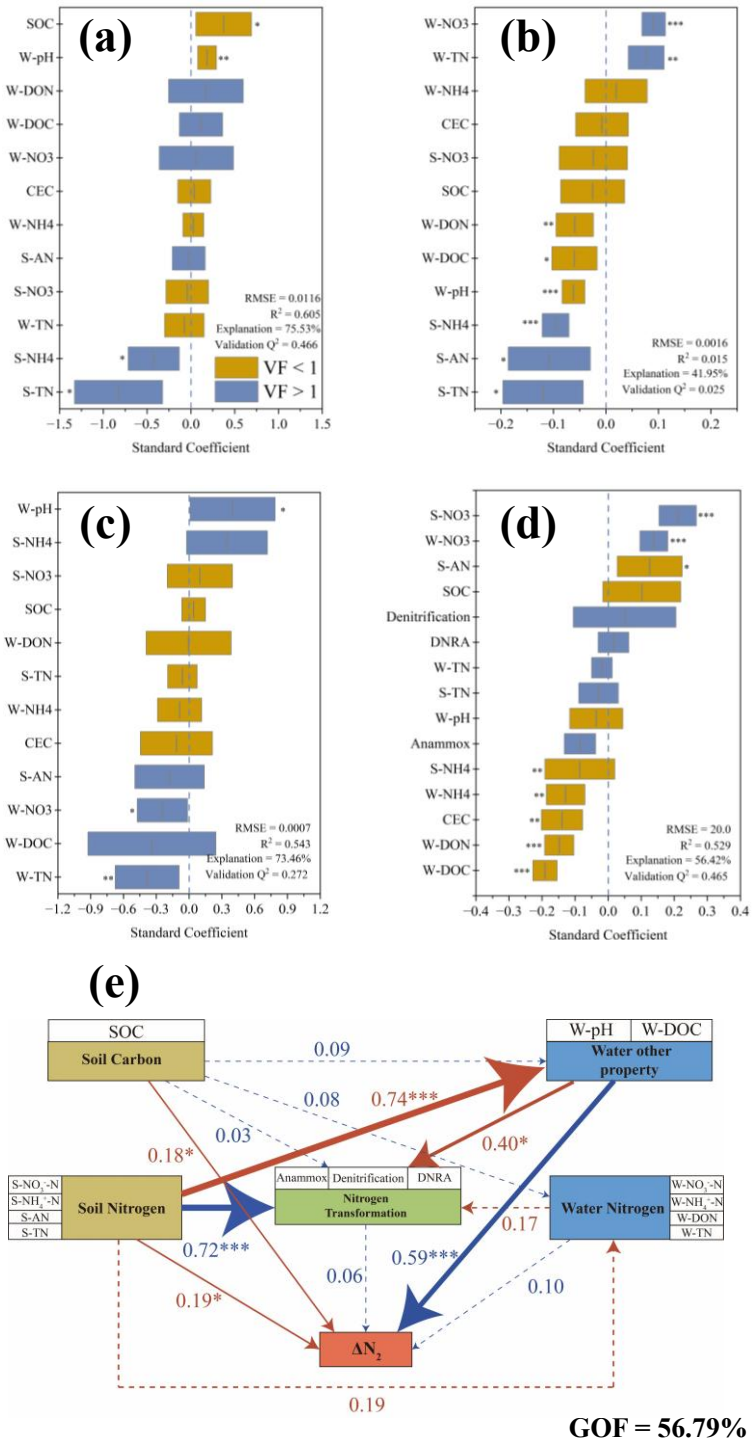

Fig. 5 Partial least squares analysis identifying the main drivers of (a) denitrification (b)Anammox (c) DNRA and (d) ΔN_2 under water and soil physicochemical properties. Partial least squares path modeling (PLS-PM) showed the effects of water and soil properties by fertilization type and flooding time on (e) ΔN_2. "Soil Nitrogen" is a latent variable indicated by S- NO_3^--N (soil NO_3^--N, "S-" denotes indicators of soil physicochemical properties), S-NH_4^+-N, S-AN and S-TN. "Soil other property" is a latent variable indicated by SOC. "Water Nitrogen" is a latent variable indicated by W- NO_3^--N (water NO_3^--N, "W-" denotes indicators of water physicochemical properties), W- NH_4^+-N, W-DON and W-TN. "Water other property" is a latent variable indicated by W-pH and W-DOC

Also “Nitrogen Transformation” is a latent variable indicated by Denitrification, Anammox and DNRA. Values adjoining the arrows represent the standardized path coefficients, and arrow widths are scaled proportionally to the path coefficients. *P < 0.05, **P < 0.01, ***P < 0.001. Blue and orange arrows denote negative and positive correlations, respectively. Dotted lines indicate paths without statistical significance (P > 0.05). GOF is the goodness of fit, a metric of the model's predictive power.

5. Conclusions

This study reveals how agricultural management intensity, represented by fertilizer type, and flooding duration jointly modulate soil nitrogen (N) transformation processes, rates, and N release at the soil–water interface in the WLFZs of the Danjiangkou Reservoir. Compared with conventional fertilizer, both controlled-release fertilizer (MP) and nitrification inhibitor (MQ) reduced dissolved inorganic nitrogen release rates into the overlying water, reflecting a lower N release intensity. However, MP, while continuously releasing NH_4^+, also introduced organic carbon, which initially stimulated denitrification but, under long-term flooding conditions, shifted toward heterotrophic DNRA as the dominant process; MQ, on the other hand, continuously inhibits nitrification, limiting the supply of NO_3^- required for denitrification and thereby promoting nitrogen retention. Flooding duration further modulated these process rates, short-term flooding followed by drying significantly enhanced denitrification potential, shifting the metabolic balance from N-conserving DNRA toward N-releasing denitrification; whereas prolonged flooding consistently promoted DNRA, reducing N release rates. Furthermore, the dynamic changes in ΔN_2 effectively reflect the competitive balance between denitrification and DNRA, a balance driven by NO_3^- supply and the availability of organic carbon. Taken together, these findings demonstrate that fertilizer type shapes nitrogen transformation pathways, while the hydrological regime regulates nitrogen release fluxes. Collectively, these findings demonstrate that fertilizer management intensity shapes the dominant N transformation pathway, while the hydrological regime regulates the corresponding transformation rates and N release fluxes. We emphasize the need to incorporate fertilizer specific carbon–nitrogen coupling in agricultural management of WLFZs, and we recommend

prioritizing new generation fertilizers with lower N-release intensity in the agricultural use of these zones to mitigate the risk of N release during reservoir impoundment periods.

Acknowledgments

This work was supported by grants from the National Natural Science Foundation of China (Grant No. U22A20562), National Key Research and Development Program of China (2024YFD1702004), the Sichuan Science and Technology Program (Grant No. 2025ZYD0008) and Research and Demonstration Project on Green Farming Models in the Riparianzone of the Danjiangkou Reservoir (ZSY/YG-ZX (2024) 030).

Reference

Avery, B.W. and Bascomb, C.L. 1974. Soil survey laboratory methods. Harpenden.

Bernardo, J.W.Y., Mannich, M., Hilgert, S., Fernandes, C.V.S. and Bleninger, T. 2017. A method for the assessment of long-term changes in carbon stock by construction of a hydropower reservoir. Ambio 46(5), 566-577.

Bordoloi, N., Baruah, K.K. and Hazarika, B. 2020. Fertilizer management through coated urea to mitigate greenhouse gas (N(2)O) emission and improve soil quality in agroclimatic zone of Northeast India. Environmental Science and Pollution Research 27(11), 11919-11931.

Bushong, J.T., Roberts, T.L., Ross, W.J., Norman, R.J., Slaton, N.A. and Wilson, C.E. 2008. Evaluation of Distillation and Diffusion Techniques for Estimating Hydrolyzable Amino Sugar-Nitrogen as a Means of Predicting Nitrogen Mineralization. Soil Science Society of America Journal 72(4), 992-999.

Cai, Y.J., Zhang, H.Y., Hu, X.R., Yang, Y.C., Hazard, C., Nicol, G.W., He, J.Z., Shen, J.P., He, Z.Y., Zhang, L., Zhang, J.H., Liu, H., Zhang, S. and Chen, Z. 2025. Millimeter-scale niche differentiation of N-cycling microorganisms across the soil-water interface has implications for N2O emissions from wetlands. The ISME journal 19(1).

Chen, M., Chang, L., Zhang, J., Guo, F., Vymazal, J., He, Q. and Chen, Y. 2020. Global nitrogen input on wetland ecosystem: The driving mechanism of soil labile carbon and nitrogen on greenhouse gas emissions. Environmental science and ecotechnology 4, 100063.

Cheng, Y., Elrys, A.S., Merwad, A.M., Zhang, H., Chen, Z., Zhang, J., Cai, Z. and Muller, C. 2022. Global Patterns and Drivers of Soil Dissimilatory Nitrate Reduction to Ammonium. Environmental Science & Technology 56(6), 3791-3800.

Cui, R., Qi, M., Fu, B., Zhao, X., Yan, H., Li, Z., Hu, W. and Chen, A. 2026. Organic material application holds great potential for alleviating soil nitrogen loss from cropland caused by shallow groundwater table fluctuations but increases N(2)O emissions. Water Research 292, 125290.

Deng, D., He, G., Ding, B., Liu, W., Yang, Z. and Ma, L. 2024. Denitrification dominates dissimilatory nitrate reduction across global natural ecosystems. Global Change Biology 30(3), e17256.

Du, F., Yin, Y., Zhai, L., Zhang, F., Wang, S., Liu, Y., Fan, X. and Liu, H. 2024. Increased anaerobic conditions promote the denitrifying nitrogen removal potential and limit anammox substrate acquisition within paddy irrigation and drainage units. Science of The Total Environment 951.

Duan, L., Fan, J., Wang, Y., Wu, Y., Xie, C., Ye, F., Lv, J., Mao, M. and Sun, Y. 2023. Interaction mechanism between nitrogen conversion and the microbial community in the hydrodynamic heterogeneous interaction zone. Environmental Science and Pollution Research 30(3), 5799-5814.

Enanga, E.M., Casson, N.J., Fairweather, T.A. and Creed, I.F. 2017. Nitrous Oxide and Dinitrogen: The Missing Flux in Nitrogen Budgets of Forested Catchments? Environmental Science & Technology 51(11), 6036-6043.

Fadum, J., Sun, X. and Zakem, E. 2025. Redox-constrained microbial ecology dictates nitrogen loss versus retention. ISME Communications 5(1), ycaf219.

Feyisa, D.S. 2026. Effects of nitrification inhibitors on crop productivity, mineral nitrogen concentrations, and gaseous emissions under field conditions: A meta-analysis of recent decades. Journal of Agriculture and Food Research 27.

Gao, J., Liu, G., Li, X., Tang, M., Cao, X., Zhou, Y. and Song, C. 2022. Organic carbon quantity and composition jointly modulate the differentiation of nitrate reduction pathways in sediments of the Chinese eutrophic lake, Lake Chaohu. Water Research 220, 118720.

Gao, Y., Song, X., Liu, K., Li, T., Zheng, W., Wang, Y., Liu, Z., Zhang, M., Chen, Q., Li, Z., Li, R., Zheng, L., Liu, W. and Miao, T. 2021. Mixture of controlled-release and conventional urea fertilizer application changed soil aggregate stability, humic acid molecular composition, and maize nitrogen uptake. Science of the Total Environment 789, 147778.

Hao, Y., Zheng, T., Liu, L., Li, P., Ma, H., Zheng, Z., Zheng, X. and Luo, J. 2025. Occurrence of dissimilatory nitrate reduction to ammonium (DNRA) in groundwater table fluctuation zones during dissolved organic nitrogen leaching through unsaturated zone. Journal of Hazardous Materials 489, 137501.

Jariwala, H., Santos, R.M., Lauzon, J.D., Dutta, A. and Wai Chiang, Y. 2022. Controlled release fertilizers (CRFs) for climate-smart agriculture practices: a comprehensive review on release mechanism, materials, methods of preparation, and effect on environmental parameters. Environmental Science and Pollution Research 29(36), 53967-53995.

Jia, M., Winkler, M.K.H. and Volcke, E.I.P. 2020. Elucidating the Competition between Heterotrophic Denitrification and DNRA Using the Resource-Ratio Theory. Environmental Science & Technology 54(21), 13953-13962.

Jiang, X., Liu, C., Cai, J., Hu, Y., Shao, K., Tang, X., Gong, Y., Yao, X., Xu, Q. and Gao, G. 2023. Relationships between environmental factors and N-cycling microbes reveal the indirect effect of further eutrophication on denitrification and DNRA in shallow lakes. Water Research 245.

Khan, A., Tan, D.K.Y., Munsif, F., Afridi, M.Z., Shah, F., Wei, F., Fahad, S. and Zhou, R. 2017. Nitrogen nutrition in cotton and control strategies for greenhouse gas emissions: a review. Environmental Science and Pollution Research 24(30), 23471-23487.

Lam, S.K., Suter, H., Mosier, A.R. and Chen, D. 2017. Using nitrification inhibitors to mitigate agricultural N(2) O emission: a double-edged sword? Global Change Biology 23(2), 485-489.

Laursen, A.E. and Seitzinger, S.P. 2002. Measurement of denitrification in rivers: an integrated, whole reach approach. Hydrobiologia 485(1-3), 67-81.

Lee, L.C., Weigelhofer, G., Hein, T., Chan, S.C., Liou, Y.S., Liao, C.S., Shiah, F.K., Yu, Y.L., Lee, T.Y. and Huang, J.C. 2023. Transition of carbon-nitrogen coupling under different anthropogenic disturbances in subtropical small mountainous rivers. Science of The Total Environment 870, 162017.

Lian, T., Cheng, L., Liu, Q., Yu, T., Cai, Z., Nian, H. and Hartmann, M. 2023. Potential relevance between soybean nitrogen uptake and rhizosphere prokaryotic communities under waterlogging stress. ISME Communications 3(1), 71.

Liu, C., Du, Y., Chen, K., Ma, S., Chen, B. and Lan, Y. 2019. Contrasting exchanges of nitrogen and phosphorus across the sediment-water interface during the drying and re-inundation of littoral eutrophic sediment. Environmental Pollution 255(Pt 3), 113356.

Liu, F., Lakshmanan, P., Zou, W., Lang, M., Li, Z.L., Zhang, F., Liang, T., Chen, J., Wang, Y., Wang, X. and Chen, X. 2025. The regulatory mechanism controlling nitrification inhibitors-induced mitigation of nitrification and NO(3)(-)-N leaching in alkaline purple soil. Journal of Environmental Management 375, 124167.

Liu, X., Zhang, Y., Li, X., Fu, C., Shi, T. and Yan, P. 2018. Effects of influent nitrogen loads on nitrogen and COD removal in horizontal subsurface flow constructed wetlands during different growth periods of Phragmites australis. Science of The Total Environment 635, 1360-1366.

Lv, K., Guo, X., Wang, C., Su, Q., Liu, D., Xiao, S. and Yang, Z. 2022. Sediment nitrogen contents controlled by microbial community in a eutrophic tributary in Three Gorges Reservoir, China. Environmental Research 314.

Maharjan, B., Vitha, S. and Okumoto, S. 2023. Developmental regulation and physical interaction among enzymes involved in sorgoleone biosynthesis. The Plant Journal 115(3), 820-832.

Miao, T., Wang, B., Wan, Y., Li, Y.e., Ren, T., Liu, H., Zhang, J., Cai, A. and Hassan, W. 2025. NH3, N2O, NO and NO2 losses, emission factors and reduction mechanisms under different N managements from greenhouse vegetable soils. Journal of Environmental Management 393.

Pang, Y. and Ji, G. 2019. Biotic factors drive distinct DNRA potential rates and contributions in typical Chinese shallow lake sediments. Environmental Pollution 254(Pt A), 112903.

Qiu, Y., Felix, J.D., Murgulet, D., Wetz, M. and Abdulla, H. 2024. Isotopic compositions of organic and inorganic nitrogen reveal processing and source dynamics at septic influenced and undeveloped estuary sites. Science of The Total Environment 925.

Riya, S., Takeuchi, Y., Zhou, S., Terada, A. and Hosomi, M. 2017. Nitrous oxide production and mRNA expression analysis of nitrifying and denitrifying bacterial genes under floodwater disappearance and fertilizer application. Environmental Science and Pollution Research 24(18), 15852-15859.

Sanchez-Rodriguez, A.R., Hill, P.W., Chadwick, D.R. and Jones, D.L. 2017. Crop residues exacerbate the negative effects of extreme flooding on soil quality. Biology and fertility of soils 53(7), 751-765.

Sao, S., Praise, S., Nishiyama, M., Ann, V., Phung, L.D. and Watanabe, T. 2024. Response of bacterial communities and soil chemistry to flood durations and recovery phases. Environmental Science and Pollution Research 32(15), 9429-9442.

Su, R., Zhao, D., Zhang, X., Zhang, H., Cheng, J., Xu, L., Wu, Q.L. and Zeng, J. 2025. Dissimilatory nitrate reduction pathways drive high nitrous oxide emissions and nitrogen retention under the

612 flash drought in the largest freshwater lake in China. Water Research 274, 123075.
613 Su, X., Zheng, Z., Chen, Y., Wan, Y., Lyu, H. and Dong, W. 2022. Effects of carbon load on nitrate
614 reduction during riverbank filtration: Field monitoring and batch experiment. Science of the
615 Total Environment 845.
616 Sun, F., Deng, Q., Li, X., Tang, M., Ma, X., Cao, X., Zhou, Y. and Song, C. 2021. Organic carbon
617 quantity and quality jointly triggered the switch between dissimilatory nitrate reduction to
618 ammonium (DNRA) and denitrification in biofilters. Chemosphere 280, 130917.
619 Valiente, N., Jirsa, F., Hein, T., Wanek, W., Prommer, J., Bonin, P. and Gomez-Alday, J.J. 2022. The
620 role of coupled DNRA-Anammox during nitrate removal in a highly saline lake. Science of the
621 Total Environment 806(Pt 3), 150726.
622 Vega-Mas, I., Mancia, A., Maggetto, L., Murillo, H., Debaq, A., Heinesch, B., Boland, F., Krause, H.-M.,
623 Vanderschuren, H. and Thonar, C. 2025. From synthetic to biological nitrification inhibition:
624 Advancing stabilization of organic fertilizers. Soil Biology and Biochemistry 211.
625 Wang, J., Jin, W., Xie, N., Che, Z., Zhang, C., Li, X., Wu, G., Yang, S., Dong, Z. and Song, H. 2025.
626 Oxygen Availability Governs the Mitigating Effect of 3,4-Dimethylpyrazole Phosphate on
627 Nitrous Oxide Emissions from Paddy Soils under Various Water Managements. Journal
628 Agricalture Food Chemistry 73(10), 5781-5791.
629 Wang, W., Wang, T., Liu, Q., Wang, H., Xue, H., Zhang, Z. and Wang, Y. 2022. Biochar-mediated
630 DNRA pathway of anammox bacteria under varying COD/N ratios. Water Research 212,
631 118100.
632 Wang, Y., Zhong, W., Zhang, X., Cao, M., Ni, Z., Zhang, M., Li, J., Duan, Y. and Wu, L. 2024. Copper
633 pyrazole addition regulates soil mineral nitrogen turnover by mediating microbial traits.
634 Frontiers in Microbiology 15, 1433816.
635 Woodward, E.E., Edwards, T.M., Givens, C.E., Kolpin, D.W. and Hladik, M.L. 2021. Widespread
636 Use of the Nitrification Inhibitor Nitrapyrin: Assessing Benefits and Costs to Agriculture,
637 Ecosystems, and Environmental Health. Environmental Science & Technology 55(3), 1345-
638 1353.
639 Wu, L., Wang, J., Xu, H., Xu, X., Gao, H., Xu, M. and Zhang, W. 2023a. Soil organic carbon priming
640 co-regulated by labile carbon input level and long-term fertilization history. Science of the Total
641 Environment 902, 166175.
642 Wu, Y., Gan, M., Huang, X., Jiang, Z. and Liu, S. 2020. Fractions and mineralization potential of the
643 sediment organic nitrogen in Daya Bay, South China Sea: Anthropogenic influence and
644 ecological implications. Marine Pollution Bulletin 160, 111594.
645 Wu, Z., Jiang, X., Chen, J., Wang, S. and Yao, C. 2023b. Geochemistry and release risk for nutrients
646 in lake sediments based on diffusive gradients in thin films. Environmental Science and
647 Pollution Research 30(14), 40588-40607.
648 Xu, A., Liu, Z., Gao, D., Gong, X., Wang, C., Huang, Z., Zhan, X. and Liang, H. 2026. Core microbial
649 community assembly driving greenhouse gas mitigation in tidal flow constructed wetlands
650 treating polluted surface water. Journal of Environmental Management 401, 128864.
651 Yang, C., Yang, R., Feng, Y., Wang, Y., Zou, Q., Song, J., Duan, J., Li, H., Gao, X., Chen, M. and Zhang,
652 H. 2025. Microplastics affect organic nitrogen in sediment: The response of organic
653 nitrogen mineralization to microbes and benthic animals. Journal of Hazardous Materials 485.
654 Yang, N., Zhang, C., Wang, L., Li, Y., Zhang, W., Niu, L., Zhang, H. and Wang, L. 2021. Nitrogen
655 cycling processes and the role of multi-trophic microbiota in dam-induced river-reservoir

systems. Water Research 206.
Ye, H., Tang, C. and Cao, Y. 2021. Sources and transformation mechanisms of inorganic nitrogen: Evidence from multi-isotopes in a rural-urban river area. Science of the Total Environment 794.
Yu, J., Zhang, Y., Zhong, J., Ding, H., Zheng, X., Wang, Z. and Zhang, Y. 2020. Water-level alterations modified nitrogen cycling across sediment-water interface in the Three Gorges Reservoir. Environmental Science and Pollution Research 27(21), 25886-25898.
Yu, L., Zhang, Y., Wang, Y., Yao, Q. and Yang, K. 2024. Effects of slow-release nitrogen and urea combined application on soil physicochemical properties and fungal community under total straw returning condition. Environmental Research 252(Pt 1), 118758.
Zhang, M., Sun, S., Gu, X., Peng, Y., Yan, P., Huang, J.-C., He, S., Bai, X., Tian, Y. and Hu, Y. 2023b. Efficient nitrogen removal pathways and corresponding microbial evidence in tidal flow constructed wetlands for saline water treatment. Environmental Research 234.
Zhang, S., Lai, L.Y., Wang, T.X., Jin, W.L., Yi, R.R., Chen, D.Z., Jin, R.C. and Yang, G.F. 2024. Response of anammox to organics with different degradation characteristics and exposure time: Performance, sludge characteristics and bacterial community. Science of the Total Environment 951, 175650
Zhang, S., Wang, F., Wang, Y., Chen, X., Xu, P. and Miao, H. 2023a. Shifts of soil archaeal nitrification and methanogenesis with elevation in water level fluctuation zone of the three Gorges Reservoir, China. Journal of Environmental Management 339.
Zhang, S., Wang, Y., Sheng, M., Chen, X., Zhang, Z., Li, S., Qin, Y., Fu, P. and Wang, F. 2025a. Decreased stability of soil dissolved organic matter under disturbance of periodic flooding and drying in reservoir drawdown area. Science of The Total Environment 969.
Zhang, X., Cui, K., Chen, X., Wei, Z., Xie, X., Zhang, X., Zhao, Y., Lv, J. and Wang, X. 2025b. Functional microbial inoculants affect the balance of DNRA and denitrification pathways in compost amended soil. Journal of Environmental Management 394.

Supplementary Files

This is a list of supplementary files associated with this preprint. Click to download.

- Supplementarymaterial.docx
- GraphicAbstract.jpg